Comprehensive Translational Assessment of Human Induced Pluripotent Stem Cell Derived Cardiomyocytes for Evaluating Drug-Induced Arrhythmias

Ksenia Blinova[*], Jayna Stohlman MS[*], Jose Vicente[*, †,‡], Dulciana Chan[*], Lars Johannesen[*], Maria P. Hortigon-Vinagre[§, ¶], Victor Zamora[§, ¶], Godfrey Smith [§, ¶], William J. Crumb[||], Li Pang[|||], Beverly Lyn-Cook[|||], James Ross[||||], Mathew Brock[||||], Stacie Chvatal[||||], Daniel Millard[||||], Loriano Galeotti[*], Norman Stockbridge[†], and David G. Strauss[*,#]

[*]US Food and Drug Administration, Center for Devices and Radiological Health, Office of Science and Engineering Laboratories, Silver Spring, MD, 20993; [†]US Food and Drug Administration, Center for Drug Evaluation and Research, Office of New Drugs, Silver Spring, MD, 20993; [‡]BSICoS Group, Aragón Institute for Engineering Research (I3A), IIS Aragón, University of Zaragoza, Zaragoza, Spain, 50018 ; [§]University of Glasgow, Glasgow, UK; [¶]Clyde Biosciences, Glasgow, UK, G12 8QQ; [||]Zenas Technologies, Metairie, LA, 70006; [|||]US Food and Drug Administration, National Center for Toxicological Research, Division of Biochemical Toxicology, Jefferson, AR, 72079; [||||]Axion BioSystems, Atlanta, GA, 30309; [#]US Food and Drug Administration, Center for Drug Evaluation and Research, Office of Clinical Pharmacology, Silver Spring, MD, 20993

E-mail addresses: Ksenia <Ksenia.Blinova@fda.hhs.gov>; Jayna <Jayna.Stohlman@fda.hhs.gov>; Jose <Jose.Vicente@fda.hhs.gov>; Dulciana <Dulciana.Chan@fda.hhs.gov>; Lars <Lars.Johannesen@fda.hhs.gov>, Maria <Maria.Hortigon@glasgow.ac.uk>; Victor <Victor.ZamoraRodriguez@glasgow.ac.uk>; Godfrey <Godfrey.Smith@glasgow.ac.uk>; William <zenasllc@bellsouth.net>; Li <Li.Pang@fda.hhs.gov>; Beverly <Beverly.Lyn-Cook@fda.hhs.gov>; James <jross@axionbio.com>; Mathew <brockm3@gene.com>; Stacie <schvatal@axion-biosystems.com>; Daniel <dmillard@axion-biosystems.com>; Loriano <Loriano.Galeotti@fda.hhs.gov>; Norman L <Norman.Stockbridge@fda.hhs.gov>; David <David.Strauss@fda.hhs.gov>

Running Title: iPSC-CM tests for drug-induced arrhythmias

Correspondence:

Ksenia Blinova, PhD

Food and Drug Administration

Bldg. 62, Room 1208

10903 New Hampshire Ave

Silver Spring, MD 20993

Fax: 301-796-9927

Tel.: 301-796-2099

Ksenia.Blinova@fda.hhs.gov

David Strauss, MD, PhD

Food and Drug Administration

Bldg. 64, Room 2062

10903 New Hampshire Ave

Silver Spring, MD 20993

Fax: 301-796-9927

Tel.: 301-796-6323

David.Strauss@fda.hhs.gov

Abstract

Background: Induced pluripotent stem cell-derived cardiomyocytes (iPSC-CM) hold promise for assessment of drug-induced arrhythmias and are being considered for use under the Comprehensive in Vitro Proarrhythmia Assay (CiPA).

Methods and Results: We studied the effects of 26 drugs and 3 drug combinations on two commercially available iPSC-CM types using high-throughput voltage-sensitive dye (VSD) and microelectrode-array (MEA) assays being studied for the Comprehensive in Vitro Proarrhythmia Assessment (CiPA) initiative and compared the results to clinical QT prolongation and torsade de pointes (TdP) risk. Concentration-dependent analysis comparing iPSC-CMs to clinical trial results demonstrated good correlation between drug-induced APDc and FPDc prolongation and clinical trial QTc prolongation. Of 20 drugs studied that exhibit clinical QTc prolongation, 17 caused APDc prolongation (16 in Cor.4U and 13 in iCell cardiomyocytes) and 16 caused FPDc prolongation (16 in Cor.4U and 10 in iCell cardiomyocytes). Of 14 drugs that cause TdP, arrhythmias occurred with 10 drugs. Lack of arrhythmic beating in iPSC-CMs for the 4 remaining drugs could be due to differences in relative levels of expression of individual ion channels. iPSC-CMs responded consistently to hERG potassium channel blocking drugs (APD prolongation and arrhythmias) and calcium channel blocking drugs (APD shortening and prevention of arrhythmias), with a more variable response to late sodium current blocking drugs.

Conclusion: Current results confirm the potential of iPSC-CMs for proarrhythmia prediction under CiPA, where iPSC-CM results would serve as a check to ion channel and in silico modeling prediction of proarrhythmic risk. A multi-site validation study is warranted.

Key Words

CiPA, iPSC-CM, MEA, VSD, iCell, Cor.4U

Introduction

Between 1988 and 2009, 14 drugs were removed from the market worldwide as a result of their potential to induce life-threatening cardiac arrhythmias (Stockbridge *et al.* 2013). Regulatory agencies responded by requiring new drugs to be assessed for their ability to block the human ether-a-go-go (hERG) potassium channel and prolong the QT interval on the electrocardiogram (2005a; 2005b). While testing for hERG potassium channel inhibition and QT prolongation has prevented torsade de pointes (TdP) inducing drugs from reaching the market, other new drugs are dropped from development, sometimes inappropriately (Stockbridge *et al.* 2013). This may especially be true for the drugs that have multichannel effects, where the deleterious effect of hERG potassium channel block may be balanced out by the drug effect on inward currents, as is the case for several marketed drugs (e.g., verapamil also blocks L-type calcium current, ranolazine blocks late sodium current) (Johannesen *et al.* 2014). This has been the driving factor for the development of a new Comprehensive *in vitro* Proarrhythmia Assay (CiPA) (Colatsky *et al.* 2016; Fermini *et al.* 2016; Sager *et al.* 2014).

CiPA calls for a three-pronged preclinical approach. First, is to assess the effect of a drug on multiple isolated cardiac ion channels (e.g. hERG, L-type calcium, sodium) in patch clamp assays. Second, is to reconstruct the human ventricular action potential with *in silico* simulations to predict the proarrhythmic liability of the drug. Third, is to perform integrated cellular studies with human induced pluripotent stem cell-derived cardiomyocytes (iPSC-CMs). Complementary phase 1 electrocardiographic (ECG) data will then be collected with ECG biomarkers that can differentiate the effects of multichannel block (Sager *et al.* 2014).

The goal of this study was to perform a thorough characterization of the current state of iPSC-CMs technologies to predict drug pro-arrhythmic risk by assessing a large number of drugs in a blinded pre-planned study to advance regulatory science in this field. Discovery of reprogramming of somatic cells into pluripotent stem cells (Takahashi *et al.* 2007; Takahashi and Yamanaka 2006), and the

consequent development of the processes required to differentiate human iPSCs into functional human cardiomyocytes (Burridge *et al.* 2012; Kattman *et al.* 2011; Laflamme *et al.* 2007; Yang *et al.* 2008) created the basis for the growing use of iPSC-CMs for cardiotoxicity screening of drugs (Clements and Thomas 2014; Gibson *et al.* 2014; Guo *et al.* 2011; Harris *et al.* 2013; Ma *et al.* 2011; Navarrete *et al.* 2013). Here we perform a comprehensive assessment of the proarrhythmic potential of 26 drugs in two commercially available iPSC-CM cell lines. The electrophysiology response of the iPSC-CMs is assessed with microelectrode arrays (MEA) and optical imaging of voltage sensitive dyes (VSD), technologies under consideration for inclusion in the CiPA screening paradigm due to promising preliminary correlation for clinically arrhythmogenic compounds (Clements and Thomas 2014; Harris *et al.* 2013). With these technologies, we focus on their ability to measure prolonged repolarization – action potential duration (APD) with VSD and field potential duration (FPD) by MEA – and detect the presence of arrhythmic events *in vitro*.

Unique to this study, we compare the iPSC-CM results to the individual ion channel effects for the multiple ion channels being studied under CiPA and characterized expression of the corresponding encoding genes in two iPSC-CMs lines: rapidly activating delayed rectifier potassium current (IKr), encoded by hERG gene, L-type calcium current (ICaL), encoded by Cav1.2, and late sodium current (late-INa), encoded by Nav1.5, which are the 3 channels primarily affected by the drugs in this study (Crumb, Jr. *et al.* 2016). Gene expression data was also obtained for KCNQ1 gene, encoding slow voltage-gated potassium channel (IKs current). In addition, we performed a comparison between the concentration-dependent response of iPSC-CMs to 8 drugs and 3 drug combinations recently studied in clinical trials. Finally, we performed iPSC-CMs experiments with chronic exposure to drugs for up to 72 hours.

Methods

iPSC-CMs

Two commercially available iPSC-CMs cell lines were used in this study: iCell (Cellular Dynamics International) and Cor.4U (Axiogenesis AG). According to the manufacturers, iCell and Cor.4U were 100% and 95% pure iPSC-cardiomyocytes correspondingly, representing a mix of ventricular-, atrial-, and nodal-like cells (see Suppl. Methods for specific lot information).

RNA Extraction and Real-time qRT-PCR

Total RNAs of human adult left ventricle were purchased from Clontech (Mountain View, CA). Total RNAs from iCell and Cor.4U iPSC-CMs were prepared with miRNeasy Mini Kit (Qiagen, Hilden, Germany), and reverse transcribed into cDNA using RT² First Strand kits (SABiosciences/Qiagen). The Clontech total RNA was pooled from three different samples. The RNAs for iCells and Cor.4U cells were isolated from cells cultured in 3 different wells of single experiment. SYBR green-based real-time qRT-PCR was performed on the CFX96 PCR detection system (Bio-Rad, Hercules, NC, USA) with gene-specific primers (SABiosciences), mRNA expression were normalized to β-actin.

Manual Patch Clamp

Stably transfected hERG, Nav1.5 cells (HEK-293) or Cav1.2 cells (CHO) were obtained from Cytocentrics Biosciences (Rostock, Germany). Cells were maintained according to the supplier instructions. The external solution had an ionic composition of (in mM): 137 NaCl, 4 KCl, 1.8 CaCl2, 1.2 MgCl2, 11 dextrose, 10 HEPES, adjusted to a pH of 7.4 with NaOH. The internal (pipette) solution had an ionic composition of (in mM): 130 KCl; 1 MgCl2, 5 NaATP, 7 NaCl, 5 EGTA, 5 HEPES, pH=7.2 using KOH. Currents were measured at 36 ± 1°C and 0.1Hz pacing rate using the whole-cell variant of the patch-clamp method (Crumb, Jr. *et al.* 1995). After rupture of the cell membrane, current amplitude and kinetics were allowed to stabilize (3-5 min) before recordings. Currents were elicited using a

ventricular action potential waveform (Johannesen *et al.* 2016) (for hERG and Cav1.2) or a voltage waveform with a holding potential of -90 mV and pulsing to -15 mV for 40 ms (Nav1.5). Late Nav1.5 was elicited with the addition of 50 μM veratridine to the external solution and was measured at the end of the 40 ms pulse. Relative block of current amplitude was measured as peak current amplitude after a steady-state effect had been reached in the presence of drug relative to current amplitude before drug addition.

MEA and VSD recordings of drug-induced effects in iPSC-CMs

100% confluent and synchronously beating Cor.4U and iCell cardiomyocytes monolayers were maintained according to manufacturer's instructions (Suppl. Methods) and assayed using an MEA system (Maestro, Axion BioSystems, Atlanta, GA) and a VSD system (CellOPTIQ, Clyde Biosciences, UK) at 37°C and 5% CO_2. MEA and VSD recordings were performed 10-14 days post-thaw in iCell cardiomyocytes and 5-10 days post-thaw in Cor.4U cardiomyocytes. Drug effects were studied in serum-free conditions at 4 doses (Suppl. Table I) by increasing drug concentration in the same well ($N \geq 3$ wells) in acute experiments (up to 5h drug exposure time, Suppl. Fig. I) or by applying a single dose in each well in chronic experiments (up to 72h). Positive (dofetilide, lidocaine, and diltiazem) and negative (untreated and vehicle, 0.1% dimethyl sulfoxide) controls were repeated on each plate. Extracellular FPD and cellular membrane APD data was recorded and analyzed off-line using AxIS (Axion Biosystems) and CellOPTIQ (Clyde Biosciences) software, respectively. The Fridericia formula(Fridericia 2003) was used to correct APD and FPD dependence on beating rate (Suppl. Fig. II) (Johannesen *et al.* 2014). Vehicle- and baseline-corrected APD at 90% repolarization (ΔΔAPD90c) and field potential duration (ΔΔFPDc) were calculated for the drugs at each dose and used to compare with the similarly calculated clinical ΔΔQTc (Johannesen *et al.* 2014; Johannesen *et al.* 2016). Drug-induced arrhythmias were monitored with both platforms (Fig. 1). VSD-recorded arrhythmias were classified into 4 categories: Type A (single

notch), Type B (multiple notches), Type C (ectopic beat) and Type T (tachyarrhythmic). In the MEA dataset, corresponding arrhythmic events (Asakura *et al.* 2015) were collectively identified as "arrhythmic beats", as shown in Fig. 1. In both MEA and VSD recordings, it was observed that some of the tested drugs inhibited spontaneous beating in the cells leading to a "quiescent" state (Q). The operators of MEA and VSD systems were blinded to treatment at the time of the recordings and data analysis.

Statistical Analysis

MEA and VSD data were analyzed using a linear-mixed effects model, where the data from untreated and vehicle control were combined and used as control. The differences for each dose were reported as the least-squares mean (95% confidence interval) of the difference between that dose and the corresponding time-matched control, using PROC MIXED in SAS 9.2 (SAS Institute, Cary, NC). A linear mixed-effects model was used to quantify the relationship between QTc and plasma drug concentration with concentration as a fixed effect and subject as a random effect on intercept and concentration.

Results

Baseline Electrophysiological Characteristics of iPSC-cardiomyocytes

iPSC-CMs selected for this study exhibited spontaneous membrane depolarization. Baseline electrophysiological characteristics of spontaneous beating in Cor.4U and iCell cardiomyocytes are summarized in the Suppl. Table II. Briefly, Cor.4U beat faster (mean beat period of 1036±55 ms from MEA and 1271±244 ms from VSD) than iCells (mean beat period of 1578±109 ms from MEA and 1876±240 ms from VSD). Cor.4U-cardiomyocytes also had shorter APD90c (299±17 ms in Cor.4U and 463±31 ms in iCells) and FPDc (299±14 ms in Cor.4U and 468±42 ms in iCells). However, as noted above, the beat rate and FPDc vs. APDc90 measurements for each cell type were very similar between MEA and VSD assays. Inter-assay and intra-assay co-efficient of variations are shown in Suppl. Table III.

Ion Channel Gene Expression

The main ion channel currents (with corresponding gene and channel names) affected by the drugs selected for the current study were IKr (KCNH2; hERG), ICaL (CACNA1C; Cav1.2), INa (SCN5A; Nav1.5) and IKs (KCNQ1/minK; KvLQT1). NaV1.5 channel is responsible for both, peak sodium current, (peak-INa, not TTX-sensitive) and the late sodium current, (late-INa, TTX-sensitive). As we recently reported, the effect of the selected drugs on the other ion channels was minimal(Crumb, Jr. *et al.* 2016). We compared the expression of the genes encoding these four channels to the expression levels in adult primary human ventricular cardiomyocytes (Fig. 2). For outward IKr current, iCells had less and Cor4.U had more hERG expression than adult cardiomyocytes, while both iPSC-CM cell types had less KCNQ1 expression (outward IKs current). For inward currents (ICaL and INa), both iCells and Cor4.U had more Cav1.2 gene expression and less Nav1.5 gene expression than adult cardiomyocytes. The differences in hERG and Cav1.2 expression between iCells and Cor4.U are consistent with iCells having a longer APD than Cor4.U at baseline, as less outward current (IKr) and more inward current (ICaL) should both contribute to a longer APD.

Effects of Dofetilide, Quinidine, Moxifloxacin, Ranolazine and Verapamil on iPSC-cardiomyocytes, and Comparison to Clinical QTc

For these five drugs, we compared *in vitro* data with the information obtained in two recent FDA-sponsored clinical trials (Johannesen *et al.* 2014; Johannesen *et al.* 2016). Representative MEA and VSD profiles in Cor.4U and iCell cardiomyocytes before and after drug addition for the five drugs are shown in Suppl. Fig. III. The iPSC-CM response (ΔΔAPDc and ΔΔFPDc, and arrhythmias) is shown in Fig. 3, along with the corresponding clinical QTc response and ion channel blockade dose-response relationships from patch clamp experiments with ion channels underlying 3 ventricular currents: hERG (IKr), Cav1.2 (ICaL), and Nav1.5 (late-INa). Data for all drugs studied in the acute experiments is provided in Suppl. Fig. IV (A-Y).

Dofetilide, a drug associated with well-characterized clinical QTc prolongation and TdP (PFIZER 1999), and which blocks hERG potassium channel exclusively in the tested dose range, induced a concentration-dependent prolongation of APDc and FPDc as well as arrhythmias in both Cor.4U and iCells. The degree of APDc and FPDc prolongation in iPSC-CMs was greater than that for clinical QTc. *In vitro* arrhythmias occurred at doses ≥2 nM, the approximate Cmax from the clinical trial (Johannesen *et al.* 2014). At the highest studied dofetilide dose (6 nM, ~3xCmax), both cell types exhibited arrhythmic beating in both VSD and MEA recordings. Of note, different patterns of arrhythmic beating occurred in the different cell types (see table inserts on Suppl. Fig. IV for the summary of observed arrhythmias). iCells first developed early afterdepolarizaions (EADs) (Figure 1: Type A arrhythmia), escalating to multiple EADs (Type B) and then ectopic beats (Type C), whereas Cor.4U cardiomyocytes preferentially developed tachyarrhythmic behavior (Type T arrhythmia).

Like dofetilide, quinidine is associated with clinical QTc prolongation and TdP (PHARM RES ASSOC 1999). Quinidine induced a dose-dependent increase in APDc and FPDc in both iCell and Cor.4U cardiomyocytes (Fig.3). No arrhythmias occurred at the first dose (300 nM), but at 900 nM (~clinical Cmax) arrhythmias were detected in both MEA and VSD signals for 100% (6/6) of wells containing iCells, but not for those with Cor.4U cardiomyocytes. At the highest studied dose (5.4 μM, or ~6.4x Cmax), all wells of the iPSC-CMs showed either arrhythmias or a cessation of spontaneous beating. The patch clamp data supports that the effect of quinidine on iPSC-CMs results primarily from hERG potassium channel block in the studied concentration range.

At standard clinical concentrations moxifloxacin induces ~5% hERG potassium channel block and 10 ms of QTc prolongation (Florian *et al.* 2011), and in our clinical study (Johannesen *et al.* 2016) a supratherapeutic dose of intravenous moxifloxacin caused a QTc prolongation of 30 ms. At similar concentrations, the iPSC cardiomyocytes did not show statistically significant APDc or FPDc

prolongation, but moxifloxacin caused concentration-dependent APDc and FPDc prolongation above this range (21-200 μM), and arrhythmias were detected in in both cell types at ~50 fold clinical Cmax.

Ranolazine causes strong block of channels underlying both the IKr (hERG) and late-INa (Nav1.5) currents (Fig. 3), which likely explain its minimal clinical risk of TdP despite QTc prolongation (Antzelevitch *et al.* 2004; Chaitman *et al.* 2004; Gilead Sciences 2013). Ranolazine caused a dose-dependent increase in APDc and FPDc in both iCell and Cor.4U cardiomyocytes (Fig. 3), but consistent with clinical observations did not induce any arrhythmias in iPSC-CMs at doses up to 15 μM (~8x Cmax). Arrhythmias were detected in 1 out of 3 replicates by MEA recordings at 23 μM (~12x Cmax). Of note, the similar levels of hERG potassium channel block induced by 2-3 nM dofetilide and 6.9 μM ranolazine (~52%) induced >200 ms of APDc and FPDc prolongation and multiple arrhythmic events in dofetilide-treated cells, but only APDc and FPDc prolongation (<150 ms) without arrhythmias in ranolazine-treated cells.

Verapamil in particular represents a case where multichannel drug-induced effects likely underlie the clinical safety. Verapamil causes strong hERG potassium channel block, and even more potent L-type calcium channel block (Fig. 3). Even at hERG channel block of ~75 %, no arrhythmias were observed in iPSC-CMs. The Cor.4U cells stopped beating at ≥150 nM, likely due to strong ICaL block. In iPSC-CMs, verapamil caused significant concentration-dependent APDc and FPDc shortening in both cell types, while no QTc shortening was observed in the clinical study (Johannesen *et al.* 2014). This is likely due to the greater sensitivity of iPSC-CMs to ICaL block, consistent higher expression of Cav1.2 compared to human adult left ventricle. The higher doses of verapamil studied in iPSC-CMs were also much greater than clinical concentrations.

Summary Results of 25 Drugs Studied in Acute Experiments

Figure 4 and 5 summarize effects of all drugs on APDc (Fig. 4) and FPDc (Fig. 5) for iCell and Cor.4U cardiomyocytes. The drugs are ordered from top to bottom from the most APDc and FPDc prolongation to the most APDc and FPDc shortening at the clinical Cmax concentration when averaged across the four combinations of platform and cell type. For each drug, the effect at clinical Cmax and the maximum effect observed at any concentration are shown. Of note, quinidine, dofetilide, quinine and ranolazine had the most APDc and FPDc prolongation at clinical concentrations, consistent with greatest hERG block at Cmax. Diltiazem and verapamil had the most APDc and FPDc shortening at clinical concentrations, consistent with substantial ICaL block.

Figure 6 shows the lowest concentration relative to clinical Cmax where cells exhibited arrhythmias and stopped beating. The drugs are ordered based on APDc and FPDc effects at Cmax as in Figures 4 and 5, and in general drugs with greater APDc and FPDc prolongation at Cmax became arrhythmic at lower concentrations. For example, quinidine, dofetilide and quinine all developed arrhythmias close to Cmax concentrations. At a given dose, Cor.4U cells were more likely to stop beating than iCells, however this was often at >50x Cmax concentrations.

The majority of arrhythmias in iPSC-CMs occurred with 60-80% hERG channel block. This is illustrated in Suppl. Fig. V, which shows the amount of hERG block present at the drug concentration where arrhythmias first developed. Notable drugs that exhibited strong hERG channel block (i.e. >60%) at higher concentrations but did not develop arrhythmias include ritonavir, mibefradil, bepridil, chlorpromazine, amitriptyline, terfenadine, amiodarone, azithromycin and verapamil. With the exception of bepridil and azithromycin, all of those drugs caused Cav1.2 or Nav1.5 (late) block (>50%). This is consistent with ICaL and late-INa block preventing hERG-related EADs and arrhythmias.

Comparison of acute effects of 25 drugs to FDA labels for QTc prolongation and TdP Risk

Of 17 drugs with an FDA label of QTc prolongation studied in the acute iPSC-CM experiments, 14 caused APDc prolongation and 13 caused FPDc prolongation in at least one iPSC-CMs type (Table 1). None of the 6 drugs without QTc prolongation on the FDA label caused FPDc or APDc prolongation. Diltiazem and verapamil shortened FPDc and APDc in both cell types and mibefradil shortened FPDc and APDc in iCell cardiomyocytes at the higher drug doses.

Of the 12 drugs with TdP risk indicated on FDA labels, arrhythmias were detected in at least one iPSC-CM type for 7 drugs for both platforms, but often at a concentration greater than standard clinical Cmax. Five drugs that have TdP risk on the FDA label, but did not cause arrhythmias in iPSC-CMs even at doses significantly exceeding clinical, were amiodarone, azithromycin, bepridil, chlorpromazine, and terfenadine. The absence of arrhythmias for amiodarone, chlorpromazine, and bepridil in iPSC-CMs may be related to potent ICaL block (Suppl. Fig. IV), and higher-than-native expression levels of Cav1.2 in iPSC-CMs (Fig. 2).

Cibenzoline and sertindole have not been approved in the U.S., however published clinical data exists showing clinical QTc prolongation for both, and TdP risk for sertindole.(Redfern *et al.* 2003) Cibenzoline induced FPDc and APDc prolongation in at least one iPSC-CM type and caused arrhythmias in iCells, but not in Cor.4U cardiomyocytes. Sertindole did not affect iCells, but induced FPDc and APDc prolongation and arrhythmias with the VSD platform in Cor.4U cells.

Of the 11 drugs that do not have TdP risk on the FDA label, arrhythmias were detected for only 2: by MEA with nilotinib for both cell types and by VSD for iCells, and for ranolazine in MEA for iCells. However this occurred only at concentrations exceeding clinical by 12 fold for ranolazine and 100 fold for nilotinib.

Overall, iPSC-CMs assay demonstrated 100% specificity (none of the clinically safe drugs induced APD/FPD prolongation in the studied dose range), 79% sensitivity for Cor.4U cardiomyocytes on both platforms, 63% for iCells on VSD and 47% for iCell on MEA platform (see Suppl. Table IV for

details on sensitivity and specificity calculation). These results suggest that while the general response to the studied drugs in all 4 cell type/combinations were similar, there was variation between the two cell types.

Drug Combinations – hERG, late sodium and calcium channel block

Co-application of drugs that block outward ionic currents (i.e. late-INa or ICaL) to balance QTc prolongation due to hERG blockade was tested in our recent clinical study (Johannesen *et al.* 2016). To see whether such effects could be observed *in vitro*, we studied the ability of the late-INa blockers lidocaine and mexiletine and ICaL blocker diltiazem to remediate the effect of IKr block from dofetilide and moxifloxacin in iPSC-CMs. Diltiazem caused substantial reversal of moxifloxacin-induced APDc and FPDc prolongation, and eliminated arrhythmias (Fig. 7). This effect did not occur in the clinical study; but interpretation there was confounded by the accumulation of a moxifloxacin metabolite (Johannesen *et al.* 2016). Both late-INa current blockers substantially shortened QTc prolongation from dofetilide in our recent clinical study (Johannesen *et al.* 2016). In iPSC-CMs, late-INa block did not cause consistent shortening of APDc or FPDc or elimination of arrhythmias, although this did occur with some combinations of cell type/platform (Suppl. Fig. VI). Lidocaine and mexiletine also had little effect on APDc or FPDc on their own (Suppl. Fig III), which may be due to lower expression of Nav1.5 in iPSC-CM vs. adult left ventricle (Fig. 2).

Chronic Effects

The stability of the spontaneous beating phenotype in cultures of iPSC-CMs (Guo *et al.* 2013) allows prolonged drug exposure to be tested, a scenario that more closely parallels the repeated clinical dosing of most drugs. We thus studied the effects of 6 drugs on iPSC-CMs during chronic exposures: 72 hours post-dose in the MEA platform (Fig. 8) and 24 hours post-dose with the VSD platform (Suppl. Fig.

VII). Chronic effects of the drugs beyond 24 hours were not studied with VSD platform to avoid repeated cell staining required for the longer term recordings. Results were consistent between MEA and VSD platform at the 24 h for the studied drugs. Pentamidine, dofetilide, amiodarone, and nilotinib generally caused progressively increasing APDc and FPDc over the course of the exposure, and the rate of change generally increased with dose (Fig. 8). An exception for these compounds was that prolongation of FPDc by dofetilide showed no time dependence for Cor.4U cells. It is notable that amiodarone did not affect APDc in acute experiments, but induced APDc prolongation in both cell types after 24 hours. Effects of diltiazem and lidocaine on APDc or FPDc had no time dependence in these experiments in either cell type and diltiazem-induced ΔΔFPDc shortening decreased after longer exposure (24-72h) in both cell types (data not shown).

Discussion

This study provides a comprehensive assessment of electrophysiology and pharmacodynamic responses of two commercially-available types of human iPSC-CMs in high-throughput assays, with quantitative comparisons to data for block of isolated ion channels and effects on clinical QTc. This type of mechanistic multiparameter characterization is critical for potential regulatory implementation of iPSC-CMs under a CiPA paradigm (Colatsky *et al.* 2016; Fermini *et al.* 2016; Sager *et al.* 2014). We observed concentration-dependent responses of both APDc and FPDc similar to clinical QTc prolongation for a series of drugs in recent FDA-sponsored clinical studies(Johannesen *et al.* 2014; Johannesen *et al.* 2016). For some drugs (e.g. dofetilide and quinidine), the prolongation was greater in iPSC-CMs compared to clinical QTc prolongation. In addition, iPSC-CM arrhythmias developed at or near clinical concentrations (Fig. 6), consistent with the known torsade de pointes risk of dofetilide and quinidine (Kolb *et al.* 2008; Nagra *et al.* 2005; Reiffel 2005; Wroblewski *et al.* 2012).

An advantage of our study is the approach that was taken to drug dose selection. Whereas many previous studies test drugs in a pre-specified dose range regardless of the individual drug potency or clinical use, the lowest dose for each drug in our study was generally set to the clinical Cmax and then increased in intervals informed by pre-existing literature on individual ion channel block (Kramer *et al.* 2013). Because significant variability in assay conditions exists in the literature, we report comparisons to manual patch experiments at physiological conditions using the same protocols for 25 drugs tested in the iPSC-CM experiments(Crumb, Jr. *et al.* 2016). The ion channel data support that block of hERG, Cav1.2 and Nav1.5 (for late-INa) are most important for predicting TdP risk. In general, strong hERG block causes EADs and arrhythmias, while multichannel block involving Cav1.2 and Nav1.5 can prevent arrhythmias due to hERG blockade. Above a certain threshold for extreme hERG block (~75% block), arrhythmias or cessation of beating often develop even with multichannel block, except for instances of extremely strong Cav1.2 block (e.g. verapamil).

While our primary focus was on the potential for drugs to acutely induce prolongation of the action potential, for a subset of drugs we also monitored APDc and FPDc during sustained chronic exposures lasting 1 (VSD) or 3 (MEA) days, which may more closely approximate clinical exposure for many drugs. For 4 drugs (pentamidine, nilotinib, dofetilide, and amiodarone) we observed progressive increases during the exposure period in APDc and FPDc beyond values obtained for acute exposure. For pentamidine, this effect is consistent with the previously-described interruption of the trafficking of hERG potassium channels to the cell membrane (Kuryshev *et al.* 2005). The effect of nilotinib on spontaneous beating in IPSC-CMs has been described previously, and may be related to observed cytotoxicity during prolonged exposure (Doherty *et al.* 2013). For amiodarone, no effect was observed for acute exposure, and evolution of APDc and FPDc prolongation could thus be due to conversion to the active desethyl metabolite (Talajic *et al.* 1987). Finally drug-induced increases in relative levels of channels carrying

inward currents may also explain progressively increasing APDc and FPDc for nilotinib and dofetilide (Lu *et al.* 2012; Talajic *et al.* 1987; Yang *et al.* 2014).

Overall, of 20 drugs studied both in acute and chronic experiments (including pentamidine, not shown in Table 1) that exhibit clinical QTc prolongation, 17 caused APDc prolongation in at least one iPSC-CM type (16 in Cor.4U and 13 in iCell cardiomyocytes) and 16 caused FPDc prolongation in at least one iPSC-CM type (16 in Cor.4U and 10 in iCell cardiomyocytes). Of 14 drugs associated with TdP risk, arrhythmias were observed for 10 drugs in acute or chronic (amiodarone, pentamidine) experiments in at least one cell type-assay combination. Lack of arrhythmic beating in iPSC-CMs for the four remaining drugs associated with clinical TdP (bepridil, chlorpromazine, terfenadine, and azithromyocin), could be due to differences in relative levels of expression of individual ion channels. For example, higher expression of Cav1.2 in iPSC-CMs (vs adult ventricles) may increase the chance that the arrhythmic potential of hERG block is offset. Indeed, with the exception of azithromycin, each of these drugs shows blockade of Cav1.2 in the tested dose rage. Moreover, it should be noted that with the exception of bepridil, these drugs stopped spontaneous beating of iPSC-CMs at the highest studied doses.

The correlation between drug effects in iPSC-CMs with clinical cardiotoxic effects was observed despite the relative immaturity of current iPSC-CMs previously discussed (Hoekstra *et al.* 2012; Knollmann 2013) and also confirmed in this study (immature phenotype, spontaneous membrane depolarizations, imperfect gene profiles as compared to adult cardiomyocytes). In addition to the ion channel encoding genes presented in this study, KCNJ2 encoding inward rectifier potassium channel protein Kir2.1 (IK1 current) is known to be particularly underexpressed in iPSC-CMs(Hoekstra *et al.* 2012). Luckily, this channel is rarely affected by therapeutic drugs and the drugs in this study had a negligible effect on IK1 current (Crumb, Jr. *et al.* 2016). While human iPSC-CMs offer distinct advantages over isolated animal cardiomyocyte for drug safety assessment by providing an unlimited and

homogeneous source of human-derived cells, the development of more mature iPSC-CMs could potentially further improve predictability of the assays based on these cells.

Study Limitations

Execution of dose-response experiments through sequential addition of ascending drug doses to the same well (vs. parallel application of different doses to different wells) allows more data points to be obtained from a single well, and allows effects of all doses to be compared to a single baseline control reading. However, the longer time required to complete the full experiment increases the risk of confounding time-dependent drug effects. In addition, each dose was added every hour for the VSD study, and every 30 minutes for the MEA study, which could explain platform-specific differences for time-dependent drug effects. Based on our results on negative controls and chronic experiments with a limited subset of the drugs, we estimate these effects to be minimal for many drugs, but we cannot completely rule it out for each individual drug. Furthermore, studying only 4 doses of each drug could not be optimal for detecting drug-induced arrhythmias, it is possible that the observed cessation of spontaneous beating at the highest doses would be preceded by arrhythmic events at a lower dose in an experiment with more drug concentrations assayed. It is likely that when using these methods in real life drug candidate screening a finer grid of doses would be assayed.

Full control of the beating rate in spontaneously beating iPSC-CMs was not possible under physiological conditions (i.e. pacing at the rates below the intrinsic rate is not effective). To account for the dependence of action potential on the beating rate in iPSC-CMS an empirical formula, Bazet (Hernandez *et al.* 2016; Kim *et al.* 2010)or Fridericia (Lewis *et al.* 2015; Maddah *et al.* 2015)is usually used, that may not accurately correct for the rate dependence in the wide range of beating rates observed after drug treatments. The need for the forced rate correction would be overcome in a more mature and pure ventricular iPSC-CMs that did not demonstrate spontaneous depolarizations.

The parallel study of the drug effects on two iPSC-CMs lines studied using two different platforms would not be possible without some differences in the experimental design necessary to manage the performance of certain cell type/platform combinations. As a result, there were variations in how the experiments were performed for each of the combinations, including cell plating density, plate coating substrate, time in culture before drug studies began, cell culture media and the timing of the recordings. It is encouraging that despite the variations in the protocols the results of the study were largely consistent between 4 combinations of cell types and recording platforms.

Each of the iPSC-CMs lines used in our study originated from a single healthy donor. A single batch of the cell lines was used for all of the experiments to minimize the variability. While improving the consistency of the results, this approach does not account for the genetic predisposition of individual patients that can play a pivotal role in defining the clinical risk of arrhythmia for individual patients. In addition, drug-induced TdP often occurs in patients with pre-existing cardiac disease. iPSC-CMs used in this study do not reflect patients with pre-existing cardiac disease.

Finally, the chosen number of replicates of each drug concentration (3) represented a balance with the desire to test a large number of drugs (26) on two cell types and two different platforms. The goal of this study was to have a broad characterization of iPSC-CM physiology and pharmacology that can guide future work for best practices and verification under the CiPA initiative, where more replicates can be tested if required.

Conclusions

Concentration-dependent analysis of drug effects on spontaneous electrical activity in iPSC-CMs, using both VSD and MEA platforms, yielded good correlation between drug-induced APDc and FPDc prolongation and clinical QTc prolongation, and between the presence of *in vitro* and clinical arrhythmias, with some limitations and differences. Spontaneous action or field potentials in iPSC-CMs were

sensitive to hERG blocking drugs (causing APDc and FPDc prolongation and arrhythmias) and ICaL-blocking drugs (causing APDc and FPDc shortening and prevention of hERG-related arrhythmias), with a more variable sensitivity to blockers of late-INa. The present results, in combination with those of other recent studies, highlight iPSC-CMs as a promising new *in vitro* technology that can be included in proarrhythmia assay paradigms, such as that proposed in CiPA. While some discrepancies exist between iPSC-CM assays and clinical experience, under CiPA they would be combined with patch clamp assessment of individual ion channels and *in silico* modeling. In combination, this is likely to be a substantial improvement in efficiency and predictivity over the present focus on hERG binding and assessment of clinical QTc prolongation late in drug development. An international multi-site validation study with standardized protocols is warranted.

Supplementary Data description

1. Supplementary methods

   Detailed protocols on iPSC-CMs plating and maintenance, MEA and VSD recordings protocols;

2. Supplementary Tables

   Suppl. Table I: Cmax and drug doses selected for iPSC-CMs experiments

   Suppl. Table II: Baseline parameters characterizing spontaneous beating in iPSC-CMs

   Suppl. Table III: Inter-assay and intra-assay variation for MEA and VSD

   Suppl. Table IV: Sensitivity and specificity of the iPSC-CMs assay to predict clinical QTc prolongation

3. Supplementary Figures

   Suppl. Fig. I: Experimental protocol for MEA and VSD recordings

   Suppl. Fig. II: APD and FPD rate-dependence correction with Fridericia formula

   Suppl. Fig. III: Representative VSD and MEA profiles for dofetilide, quinidine, moxifloxacin, ranolazine, and verapamil.

   Suppl. Fig. IV: Drug-induced effects on APDc and FPDc in iPSC-CMs and drug-induced relative channel block

   Suppl. Fig. V: Minimum percent hERG block at which a drug induced arrhythmias in iPSC-CMs

   Suppl. Fig. VI: Effect of drug combinations (dofetilide+lidocaine and dofetilide+mexiletine in iPS-CMs)

   Suppl. Fig. VII: Chronic effects of pentamidine, amiodarone, dofetilide and nilotinib in iCell and Cor.4U cardiomyoyctes in VSD assay

Funding Information

This work was supported by FDA's Chief Scientist's Challenge Grant, Critical Path Initiative, FDA Office of Women's Health Grant, and appointments to the Research Participation Program at the Center for Devices and Radiological Health administered by the Oak Ridge Institute for Science and Education through an interagency agreement between the U.S. Department of Energy and the U.S. Food and Drug Administration. MPHV and VZ are recipients of Fundacion Alfonso Martin Escudero (SPAIN) postdoctoral fellowships

Acknowledgements

iPSC-CMs for this study were obtained via material transfer agreement from Cellular Dynamics International and Axiogenesis AG. All iPSC-CM experiments were performed at FDA under research collaboration agreements with Clyde Biosciences and Axion Biosystems. Patch clamp experiments were performed at Zenas Technologies. The mention of commercial products, their sources, or their use in connection with material reported herein is not to be construed as either an actual or implied endorsement of such products by the U.S. Department of Health and Human Services.

References

Reference List

1. (2005a). International Conference on Harmonisation; guidance on E14 Clinical Evaluation of QT/QTc Interval Prolongation and Proarrhythmic Potential for Non-Antiarrhythmic Drugs; availability. Notice. *Fed Regist.* **70**(202), 61134-61135.

2. (2005b). International Conference on Harmonisation; guidance on S7B Nonclinical Evaluation of the Potential for Delayed Ventricular Repolarization (QT Interval Prolongation) by Human Pharmaceuticals; availability. Notice. *Fed. Regist.* **70**(202), 61133-61134.

3. Antzelevitch, C., Belardinelli, L., Zygmunt, A. C., Burashnikov, A., Di Diego, J. M., Fish, J. M., Cordeiro, J. M., and Thomas, G. (2004). Electrophysiological effects of ranolazine, a novel antianginal agent with antiarrhythmic properties. *Circulation* **110**(8), 904-910.

4. Asakura, K., Hayashi, S., Ojima, A., Taniguchi, T., Miyamoto, N., Nakamori, C., Nagasawa, C., Kitamura, T., Osada, T., Honda, Y., Kasai, C., Ando, H., Kanda, Y., Sekino, Y., and Sawada, K. (2015). Improvement of acquisition and analysis methods in multi-electrode array experiments with iPS cell-derived cardiomyocytes. *J Pharmacol. Toxicol Methods*.

5. Burridge, P., Keller, G., Gold, J., and Wu, J. (2012). Production of De Novo Cardiomyocytes: Human Pluripotent Stem Cell Differentiation and Direct Reprogramming. *Cell Stem Cell* **10**(1), 16-28.

6. Chaitman, B. R., Pepine, C. J., Parker, J. O., Skopal, J., Chumakova, G., Kuch, J., Wang, W., Skettino, S. L., and Wolff, A. A. (2004). Effects of ranolazine with atenolol, amlodipine, or diltiazem on exercise tolerance and angina frequency in patients with severe chronic angina: a randomized controlled trial. *JAMA* **291**(3), 309-316.

7. Clements, M., and Thomas, N. (2014). High-throughput multi-parameter profiling of electrophysiological drug effects in human embryonic stem cell derived cardiomyocytes using multi-electrode arrays. *Toxicol Sci* **140**(2), 445-461.

8. Colatsky, T., Fermini, B., Gintant, G., Pierson, J. B., Sager, P., Sekino, Y., Strauss, D. G., and Stockbridge, N. (2016). The Comprehensive in Vitro Proarrhythmia Assay (CiPA) initiative - Update on progress. *J Pharmacol Toxicol Methods*. Advance Access published June 7 2016, doi: 10.1016/j.vascn.2016.06.002

9. Crumb, W. J., Jr., Pigott, J. D., and Clarkson, C. W. (1995). Description of a nonselective cation current in human atrium. *Circ. Res* **77**(5), 950-956.

10. Crumb, W. J., Jr., Vicente, J., Johannesen, L., and Strauss, D. G. (2016). An evaluation of 30 clinical drugs against the comprehensive in vitro proarrhythmia assay (CiPA) proposed ion channel panel. *J Pharmacol Toxicol Methods*. Advance Access published April 6 2016, doi: 10.1016/j.vascn.2016.03.009

11. Doherty, K. R., Wappel, R. L., Talbert, D. R., Trusk, P. B., Moran, D. M., Kramer, J. W., Brown, A. M., Shell, S. A., and Bacus, S. (2013). Multi-parameter in vitro toxicity testing of crizotinib, sunitinib, erlotinib, and nilotinib in human cardiomyocytes. *Toxicol Appl. Pharmacol.* **272**(1), 245-255.

12. Fermini, B., Hancox, J. C., Abi-Gerges, N., Bridgland-Taylor, M., Chaudhary, K. W., Colatsky, T., Correll, K., Crumb, W., Damiano, B., Erdemli, G., Gintant, G., Imredy, J., Koerner, J., Kramer, J., Levesque, P., Li, Z., Lindqvist, A., Obejero-Paz, C. A., Rampe, D., Sawada, K., Strauss, D. G., and Vandenberg, J. I. (2016). A New Perspective in the Field of Cardiac Safety Testing through the Comprehensive In Vitro Proarrhythmia Assay Paradigm. *J Biomol. Screen.* **21**(1), 1-11.

13. Florian, J. A., Tornoe, C. W., Brundage, R., Parekh, A., and Garnett, C. E. (2011). Population pharmacokinetic and concentration--QTc models for moxifloxacin: pooled analysis of 20 thorough QT studies. *J Clin. Pharmacol.* **51**(8), 1152-1162.

14. Fridericia, L. S. (2003). The duration of systole in an electrocardiogram in normal humans and in patients with heart disease. 1920. *Ann Noninvasive. Electrocardiol.* **8**(4), 343-351.

15. Gibson, J. K., Yue, Y., Bronson, J., Palmer, C., and Numann, R. (2014). Human stem cell-derived cardiomyocytes detect drug-mediated changes in action potentials and ion currents. *J Pharmacol. Toxicol. Methods* **70**(3), 255-267.

16. Gilead Sciences, I. Ranexa (Ranolazine), label information. 2013.

17. Guo, L., Abrams, R. M., Babiarz, J. E., Cohen, J. D., Kameoka, S., Sanders, M. J., Chiao, E., and Kolaja, K. L. (2011). Estimating the risk of drug-induced proarrhythmia using human induced pluripotent stem cell-derived cardiomyocytes. *Toxicol Sci* **123**(1), 281-289.

18. Guo, L., Coyle, L., Abrams, R. M., Kemper, R., Chiao, E. T., and Kolaja, K. L. (2013). Refining the human iPSC-cardiomyocyte arrhythmic risk assessment model. *Toxicol Sci.* **136**(2), 581-594.

19. Harris, K., Aylott, M., Cui, Y., Louttit, J. B., McMahon, N. C., and Sridhar, A. (2013). Comparison of electrophysiological data from human-induced pluripotent stem cell-derived cardiomyocytes to functional preclinical safety assays. *Toxicol Sci.* **134**(2), 412-426.

20. Hernandez, D., Millard, R., Sivakumaran, P., Wong, R. C., Crombie, D. E., Hewitt, A. W., Liang, H., Hung, S. S., Pebay, A., Shepherd, R. K., Dusting, G. J., and Lim, S. Y. (2016).

Electrical Stimulation Promotes Cardiac Differentiation of Human Induced Pluripotent Stem Cells. *Stem Cells Int* **2016**, 1718041.

21. Hoekstra, M., Mummery, C. L., Wilde, A. A., Bezzina, C. R., and Verkerk, A. O. (2012). Induced pluripotent stem cell derived cardiomyocytes as models for cardiac arrhythmias. *Front Physiol.* **3**, 346.

22. Johannesen, L., Vicente, J., Mason, J. W., Erato, C., Sanabria, C., Waite-Labott, K., Hong, M., Lin, J., Guo, P., Mutlib, A., Wang, J., Crumb, W. J., Blinova, K., Chan, D., Stohlman, J., Florian, J., Ugander, M., Stockbridge, N., and Strauss, D. G. (2016). Late sodium current block for drug-induced long QT syndrome: Results from a prospective clinical trial. *Clin Pharmacol Ther* **99**(2), 214-223.

23. Johannesen, L., Vicente, J., Mason, J. W., Sanabria, C., Waite-Labott, K., Hong, M., Guo, P., Lin, J., Sorensen, J. S., Galeotti, L., Florian, J., Ugander, M., Stockbridge, N., and Strauss, D. G. (2014). Differentiating drug-induced multichannel block on the electrocardiogram: randomized study of dofetilide, quinidine, ranolazine, and verapamil. *Clin Pharmacol Ther* **96**(5), 549-558.

24. Kattman, S. J., Witty, A. D., Gagliardi, M., Dubois, N. C., Niapour, M., Hotta, A., Ellis, J., and Keller, G. (2011). Stage-Specific Optimization of Activin/Nodal and BMP Signaling Promotes Cardiac Differentiation of Mouse and Human Pluripotent Stem Cell Lines. *Cell Stem Cell* **8**(2), 228-240.

25. Kim, C., Majdi, M., Xia, P., Wei, K. A., Talantova, M., Spiering, S., Nelson, B., Mercola, M., and Chen, H. S. (2010). Non-cardiomyocytes influence the electrophysiological maturation of human embryonic stem cell-derived cardiomyocytes during differentiation. *Stem Cells Dev* **19**(6), 783-795.

26. Knollmann, B. C. (2013). Induced pluripotent stem cell-derived cardiomyocytes: boutique science or valuable arrhythmia model? *Circ. Res* **112**(6), 969-976.

27. Kolb, C., Ndrepepa, G., and Zrenner, B. (2008). Late dofetilide-associated life-threatening proarrhythmia. *Int J Cardiol.* **127**(2), e54-e56.

28. Kramer, J., Obejero-Paz, C. A., Myatt, G., Kuryshev, Y. A., Bruening-Wright, A., Verducci, J. S., and Brown, A. M. (2013). MICE models: superior to the HERG model in predicting Torsade de Pointes. *Sci Rep* **3**, 2100.

29. Kuryshev, Y. A., Ficker, E., Wang, L., Hawryluk, P., Dennis, A. T., Wible, B. A., Brown, A. M., Kang, J., Chen, X. L., Sawamura, K., Reynolds, W., and Rampe, D. (2005). Pentamidine-induced long QT syndrome and block of hERG trafficking. *J Pharmacol Exp. Ther* **312**(1), 316-323.

30. Laflamme, M. A., Chen, K. Y., Naumova, A. V., Muskheli, V., Fugate, J. A., Dupras, S. K., Reinecke, H., Xu, C., Hassanipour, M., Police, S., O'Sullivan, C., Collins, L., Chen, Y.,

Minami, E., Gill, E. A., Ueno, S., Yuan, C., Gold, J., and Murry, C. E. (2007). Cardiomyocytes derived from human embryonic stem cells in pro-survival factors enhance function of infarcted rat hearts. *Nat Biotech* **25**(9), 1015-1024.

31. Lewis, K. J., Silvester, N. C., Barberini-Jammaers, S., Mason, S. A., Marsh, S. A., Lipka, M., and George, C. H. (2015). A new system for profiling drug-induced calcium signal perturbation in human embryonic stem cell-derived cardiomyocytes. *J Biomol. Screen.* **20**(3), 330-340.

32. Lu, Z., Wu, C. Y., Jiang, Y. P., Ballou, L. M., Clausen, C., Cohen, I. S., and Lin, R. Z. (2012). Suppression of phosphoinositide 3-kinase signaling and alteration of multiple ion currents in drug-induced long QT syndrome. *Sci Transl. Med* **4**(131), 131ra50.

33. Ma, J., Guo, L., Fiene, S. J., Anson, B. D., Thomson, J. A., Kamp, T. J., Kolaja, K. L., Swanson, B. J., and January, C. T. (2011). High purity human-induced pluripotent stem cell-derived cardiomyocytes: electrophysiological properties of action potentials and ionic currents. *Am J Physiol Heart Circ. Physiol* **301**(5), H2006-H2017.

34. Maddah, M., Heidmann, J. D., Mandegar, M. A., Walker, C. D., Bolouki, S., Conklin, B. R., and Loewke, K. E. (2015). A non-invasive platform for functional characterization of stem-cell-derived cardiomyocytes with applications in cardiotoxicity testing. *Stem Cell Reports* **4**(4), 621-631.

35. Nagra, B. S., Ledley, G. S., and Kantharia, B. K. (2005). Marked QT prolongation and torsades de pointes secondary to acute ischemia in an elderly man taking dofetilide for atrial fibrillation: a cautionary tale. *J Cardiovasc. Pharmacol Ther* **10**(3), 191-195.

36. Navarrete, E. G., Liang, P., Lan, F., Sanchez-Freire, V., Simmons, C., Gong, T., Sharma, A., Burridge, P. W., Patlolla, B., Lee, A. S., Wu, H., Beygui, R. E., Wu, S. M., Robbins, R. C., Bers, D. M., and Wu, J. C. (2013). Screening drug-induced arrhythmia [corrected] using human induced pluripotent stem cell-derived cardiomyocytes and low-impedance microelectrode arrays. *Circulation* **128**(11 Suppl 1), S3-13.

37. Pfizer. Tikosyn (Dofetilide), label information. 1999.

38. Pharm. Res. Assoc. Cardioquin (Quinidine Polygalacturonate), label information. 1999.

39. Redfern, W. S., Carlsson, L., Davis, A. S., Lynch, W. G., MacKenzie, I., Palethorpe, S., Siegl, P. K., Strang, I., Sullivan, A. T., Wallis, R., Camm, A. J., and Hammond, T. G. (2003). Relationships between preclinical cardiac electrophysiology, clinical QT interval prolongation and torsade de pointes for a broad range of drugs: evidence for a provisional safety margin in drug development. *Cardiovasc. Res* **58**(1), 32-45.

40. Reiffel, J. A. (2005). Atypical proarrhythmia with dofetilide: monomorphic VT and exercise-induced torsade de pointes. *Pacing Clin. Electrophysiol.* **28**(8), 877-879.

41. Sager, P. T., Gintant, G., Turner, J. R., Pettit, S., and Stockbridge, N. (2014). Rechanneling the cardiac proarrhythmia safety paradigm: a meeting report from the Cardiac Safety Research Consortium. *Am Heart. J* **167**(3), 292-300.

42. Stockbridge, N., Morganroth, J., Shah, R. R., and Garnett, C. (2013). Dealing with global safety issues : was the response to QT-liability of non-cardiac drugs well coordinated? *Drug Saf.* **36**(3), 167-182.

43. Takahashi, K., Tanabe, K., Ohnuki, M., Narita, M., Ichisaka, T., Tomoda, K., and Yamanaka, S. (2007). Induction of Pluripotent Stem Cells from Adult Human Fibroblasts by Defined Factors. *Cell* **131**(5), 861-872.

44. Takahashi, K., and Yamanaka, S. (2006). Induction of Pluripotent Stem Cells from Mouse Embryonic and Adult Fibroblast Cultures by Defined Factors. *Cell* **126**(4), 663-676.

45. Talajic, M., DeRoode, M. R., and Nattel, S. (1987). Comparative electrophysiologic effects of intravenous amiodarone and desethylamiodarone in dogs: evidence for clinically relevant activity of the metabolite. *Circulation* **75**(1), 265-271.

46. Wroblewski, H. A., Kovacs, R. J., Kingery, J. R., Overholser, B. R., and Tisdale, J. E. (2012). High risk of QT interval prolongation and torsades de pointes associated with intravenous quinidine used for treatment of resistant malaria or babesiosis. *Antimicrob. Agents. Chemother.* **56**(8), 4495-4499.

47. Yang, L., Soonpaa, M. H., Adler, E. D., Roepke, T. K., Kattman, S. J., Kennedy, M., Henckaerts, E., Bonham, K., Abbott, G. W., Linden, R. M., Field, L. J., and Keller, G. M. (2008). Human cardiovascular progenitor cells develop from a KDR+ embryonic-stem-cell-derived population. *Nature* **453**(7194), 524-528.

48. Yang, T., Chun, Y. W., Stroud, D. M., Mosley, J. D., Knollmann, B. C., Hong, C., and Roden, D. M. (2014). Screening for acute IKr block is insufficient to detect torsades de pointes liability: role of late sodium current. *Circulation* **130**(3), 224-234.

Figure Legends

Fig. 1. Arrhythmias observed in iPSC-CMs

The first five traces show VSD recordings of normal and arrhythmic iPSC-CM action potentials. Different types of arrhythmias are shown (A, B, C, and T). The last three traces represent normal MEA beating and two examples of MEA traces with arrhythmias: a notched repolarization waveform and ectopic beat.

Fig. 2. iPSC-CM ion channel gene expression profiles

Expression of the genes encoding four ion channels: SCN5A (Nav1.5), CACNA1C (Cav1.2), KCNH2 (hERG), and KCNQ1 in human primary adult cardiac tissue and human iPSC-CMs (normalized to adult primary levels). Data represent means ± SD for N=3 replicates. Stars indicate statistically significant differences ($p<0.05$).

Fig. 3. Effect of dofetilide, quinidine, moxifloxacin, ranolazine and verapamil on iPSC-CM APDc, FPDc and clinical QTc

For each drug, left panels show relative drug-induced channel block from patch clamp experiments, the error bars represent ± SE of mean percent channel block. The vertical lines represent clinical Cmax (solid line) and drug doses in iPSC-CMs experiments (dashed lines). The middle and right panels show drug-induced changes in APDc and FPDc in iCell (orange) and Cor.4U (gray), and clinical QTc (blue). 95% confidence intervals are shown as error bars in ΔΔAPDc and ΔΔFPDc and in gray shading for the clinical QTc data. The tables represent the number of wells in acute iPSC-CM experiments where drug-induced arrhythmic events or

cessation of spontaneous contractions (Q) were observed in MEA and VSD, along with the type (A, B, C, or T) of the arrhythmia (for VSD).

Fig. 4. Acute effects of 25 drugs on FPDc in iCell and Cor.4U cardiomyocytes

The two panels represent drug effects on FPDc in each cell type. The mean values for ΔΔFPDc are shown with the error bars representing 95% CI of the calculated mean across replicates (solid error bars are used for p-value <0.05, and dotted error bars are used for p-value≥0.05). The effect on APDc/FPDc at clinical Cmax (green) and the maximum effect observed at any drug concentration (red) are shown for each drug. Note that only drug doses when FPD could be measured (i.e. cells were spontaneously beating and the induced arrhythmias did not interfere with the FPDc calculations) are included. The vertical black dotted lines represent 2 SD threshold calculated for the variability in FPDc for the vehicle control wells for each cell type. The drugs are ordered from top to bottom by the drugs having the most APDc/FPDc prolongation to the most APDc/FPDc shortening at the clinical Cmax concentration when averaged among the four combinations of platform and cell type.

Fig. 5. Acute effects of 25 drugs on APD90c in iCell and Cor.4U cardiomyocytes

The two panels represent drug effects on APD90c in each cell type. The mean values for ΔΔAPDc are shown with the error bars representing 95% CI of the calculated mean across replicates (solid error bars are used for p-value <0.05, and dotted error bars are used for p-value≥0.05). The effect on APD90c at clinical Cmax (green) and the maximum effect observed at any drug concentration (red) are shown for each drug. Note that only drug doses when APD90c could be measured (i.e. cells were spontaneously beating and the induced arrhythmias did not interfere with the APD90c calculations) are included. The vertical black dotted lines

represent 2 SD threshold calculated for the variability in APD90c for the vehicle control wells for each cell type. The drugs are ordered from top to bottom by the drugs having the most APD90c/FPDc prolongation to the most APD90c/FPDc shortening at the clinical Cmax concentration when averaged among the four combinations of platform and cell type.

Fig. 6. Drug induced arrhythmias/quiescence in iCell and Cor.4U cardiomyocytes

The four panels represent drug-induced arrhythmias and inhibition of the spontaneous beating (quiescent) effects in each cell type-assay combination. The lowest drug concentration at which drug-induced arrhythmias (red crosses) or cessation of spontaneous beating (blue circles) is shown for each drug as number of folds of the clinical Cmax of that drug.

Fig. 7. Diltiazem effect on moxifloxacin-induced APDc/FPDc prolongation and arrhythmias

The four panels represent drug effects in each cell type/assay combination. Moxifloxacin was added to the iPSC-CMs at three different concentrations at the first dosing, then diltiazem was added in increasing concentrations at the three subsequent dosings while moxifloxacin concentration was maintained constant. The least-square means of drug-induced changes in FPDc and APD90c are shown with error bars representing 95% CI from the means. The symbols on the top of the graphs represent time points where either arrhythmias (open symbols) or inhibition of spontaneous beating (crosses) were observed. The color of the symbols corresponds to the color-coding of moxifloxacin concentrations (see the legend on the bottom of the plot).

Fig. 8. Chronic effects of pentamidine, amiodarone, dofetilide and nilotinib on iCell and Cor.4U cardiomyocytes in MEA assay

The mean drug-induced changes in FPDc are shown with error bars representing 95% CI from the least-square means of the differences. The symbols on the bottom of the graphs represent

time points where either arrhythmias (crosses) or inhibition of spontaneous beating (open circles) were observed. The color of these symbols corresponds to the color-coding of the drug concentrations (see the legend on the right side of each panel).

Tables

Table 1. Comparison of acute drug-induced effects in iPSC-CMs with QTc and TdP information on the corresponding FDA drug label

Drug	Repolarization effect in iPS cells				Arrhythmias induced in iPS			
	ΔΔFPDc Cor.4U	ΔΔFPDc iCell	ΔΔAPDc Cor.4U	ΔΔAPDc iCell	MEA Cor.4U	MEA iCell	VSD Cor.4U	VSD iCell
QT ↑and TdP on the FDA label								
Quinidine	↑	↑	↑	↑	×	×	-	×
Dofetilide	↑	↑	↑	↑	×	×	×	×
Quinine	↑	↑	↑	↑	-	×	×	×
Propafenone	↑	↑	↑	↑	-	×	-	×
Moxifloxacin	↑	↑	↑	↑	×	×	×	×
Chloroquine	↑	↑	↑	↑	×	×	×	×
Bepridil	↑	-	↑	↑	-	-	-	-
Chlorpromazine	-	-	↑	-	-	-	-	-
Terfenadine	↑	-	↑	↑	-	-	-	-
Cisapride	↑	↑	↑	-	×	-	-	×
Amiodarone	↑	-	-	-	-	-	-	-
Azithromycin	-	↓	-	↓	-	-	-	-
QT ↑, but no TdP on the FDA label								
Ranolazine	↑	↑	↑	↑	-	×	-	-
Ritonavir	↑	-	↑	-	-	-	-	-
Amitriptyline	-	-	-	-	-	-	-	-
Nilotinib	↑	↑	↑	↑	×	×	-	×
Toremifene	-	-	-	↑	-	-	-	-
No QT ↑, nor TdP on the FDA label								
Lidocaine	-	-	-	-	-	-	-	-
Mexiletine	-	-	-	-	-	-	-	-
Mibefradil	-	↓	-	↓	-	-	-	-
Diltiazem	↓	↓	↓	↓	-	-	-	-
Verapamil	↓	↓	↓	↓	-	-	-	-
Licarbazepine	-	-	-	-	-	-	-	-
Not FDA-cleared*								
Cibenzoline	↑	-	↑	↑	-	×	-	×
Sertindole	↑	-	↑	-	-	-	×	-

* cibenzoline (**QTc ↑),** sertindole (**QTc ↑, TdP)(Redfern *et al.* 2003)**

Table 1. Twenty-five drugs studied in acute iPSC-CM experiments are divided into four categories based on the presence of QTc prolongation and TdP reports on the FDA-approved label. Symbol ↑ means that drug induced statistically significant (p-value<0.05) and above the threshold change in APDc or FPDc for at least one of the doses. The threshold for each cell type-assay combination was set at the two standard deviations of the variability in APDc/FPDc measurements in the control (no drug) wells. Red shading represents the drugs that induced FPDc or APDc prolongation (↑) and green shading represents the drugs that shortened FPDc or APDc (↓) or had no effect. The cross symbol (×) means that the corresponding drug induced arrhythmias in at least 30% of the replicate wells.

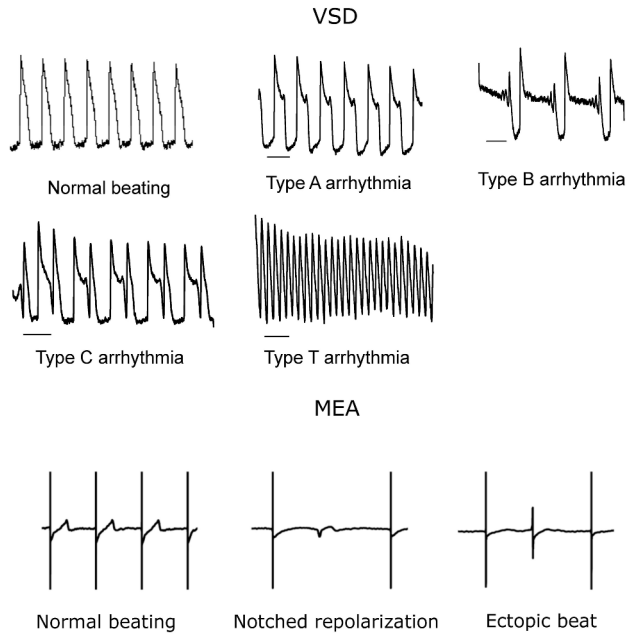

Fig. 1. Arrhythmias observed in iPSC-CMs
The first five traces show VSD recordings of normal and arrhythmic iPSC-CM action potentials. Different types of arrhythmias are shown (A, B, C, and T). The last three traces represent normal MEA beating and two examples of MEA traces with arrhythmias: a notched repolarization waveform and ectopic beat.

Fig. 1
279x361mm (300 x 300 DPI)

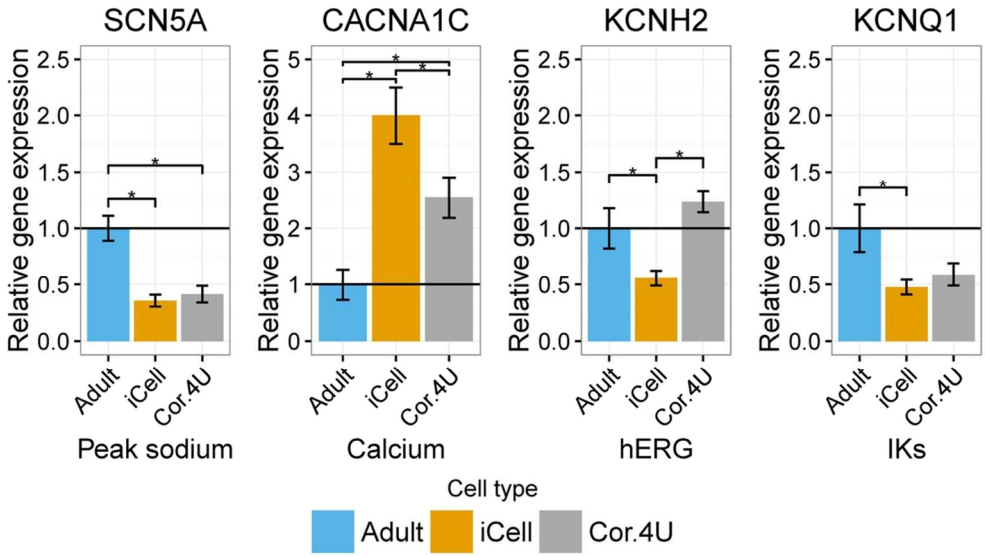

Fig. 2. iPSC-CM ion channel gene expression profiles
Expression of the genes encoding four ion channels: SCN5A (Nav1.5), CACNA1C (Cav1.2), KCNH2 (hERG), and KCNQ1 in human primary adult cardiac tissue and human iPSC-CMs (normalized to adult primary levels). Data represent means ± SD for N=3 replicates. Stars indicate statistically significant differences ($p<0.05$).

Fig. 2
100x56mm (300 x 300 DPI)

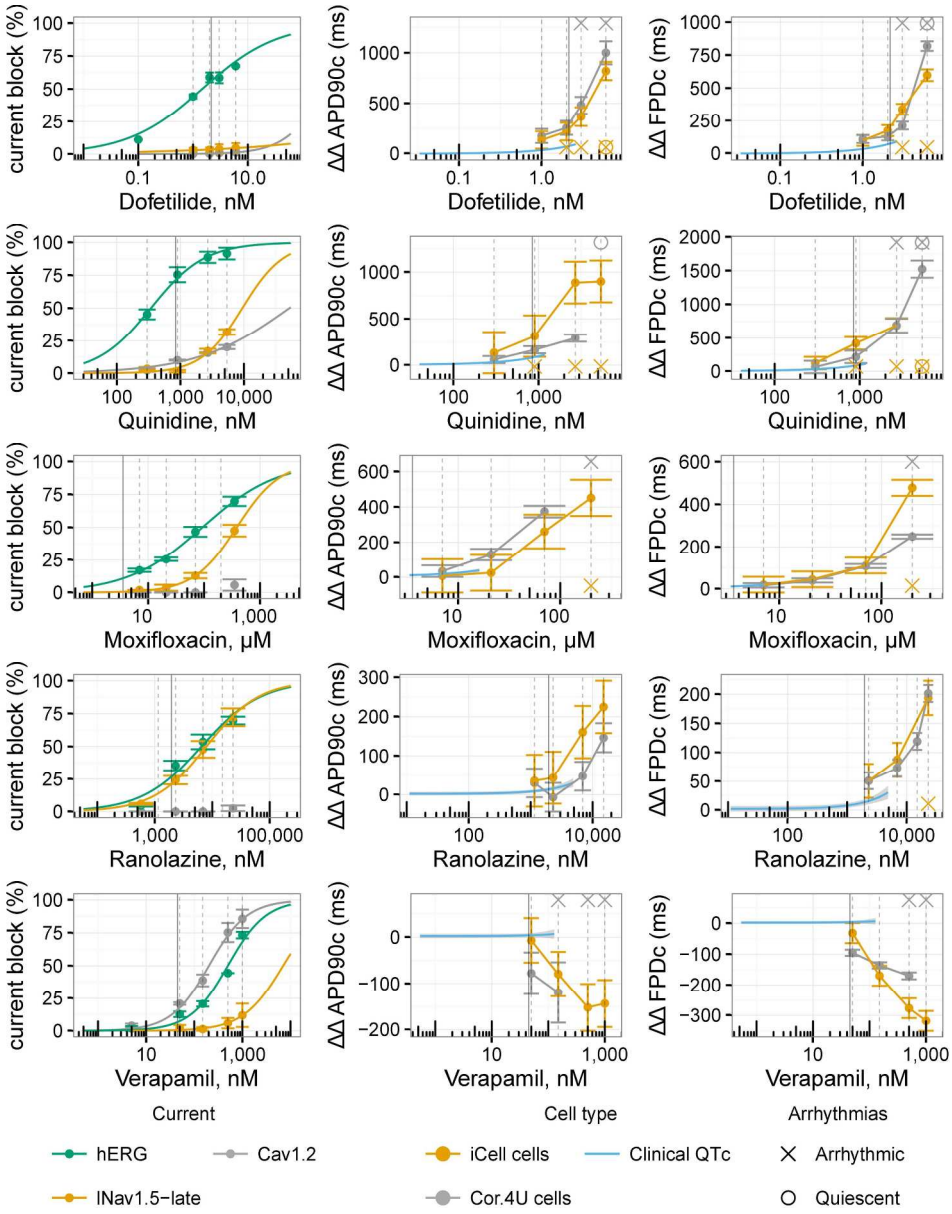

Fig. 3. Effect of dofetilide, quinidine, moxifloxacin, ranolazine and verapamil on iPSC-CM APDc, FPDc and clinical QTc

For each drug, left panels show relative drug-induced channel block from patch clamp experiments, the error bars represent ± SE of mean percent channel block. The vertical lines represent clinical Cmax (solid line) and drug doses in iPSC-CMs experiments (dashed lines). The middle and right panels show drug-induced changes in APDc and FPDc in iCell (orange) and Cor.4U (gray), and clinical QTc (blue). 95% confidence intervals are shown as error bars in ΔΔAPDc and ΔΔFPDc and in gray shading for the clinical QTc data. The tables represent the number of wells in acute iPSC-CM experiments where drug-induced arrhythmic events or cessation of spontaneous contractions (Q) were observed in MEA and VSD, along with the type (A, B, C, or T) of the arrhythmia (for VSD).

Fig. 3
225x280mm (300 x 300 DPI)

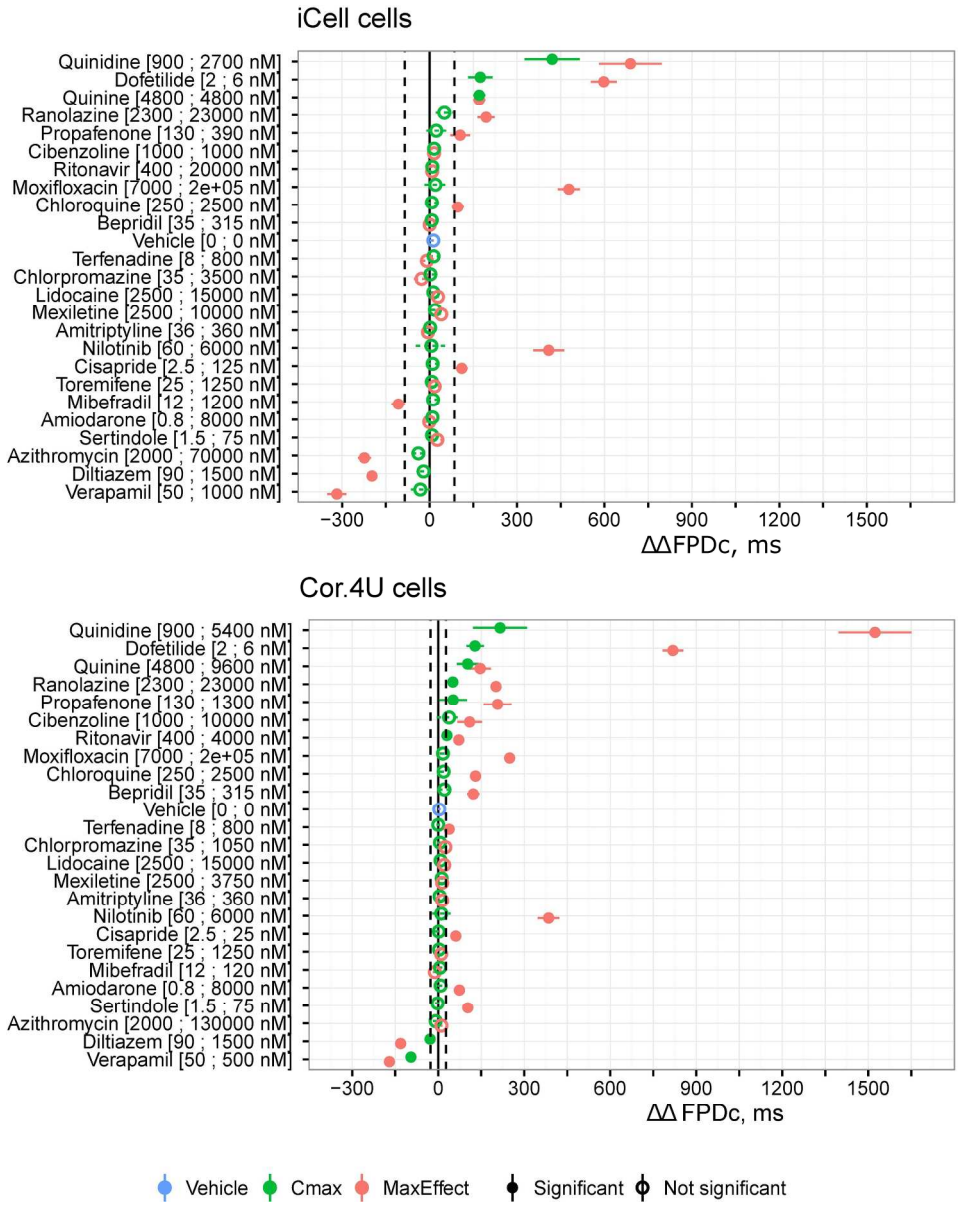

Fig. 4. Acute effects of 25 drugs on FPDc in iCell and Cor.4U cardiomyocytes
The two panels represent drug effects on FPDc in each cell type. The mean values for ΔΔFPDc are shown with the error bars representing 95% CI of the calculated mean across replicates (solid error bars are used for p-value <0.05, and dotted error bars are used for p-value≥0.05). The effect on APDc/FPDc at clinical Cmax (green) and the maximum effect observed at any drug concentration (red) are shown for each drug. Note that only drug doses when FPD could be measured (i.e. cells were spontaneously beating and the induced arrhythmias did not interfere with the FPDc calculations) are included. The vertical black dotted lines represent 2 SD threshold calculated for the variability in FPDc for the vehicle control wells for each cell type. The drugs are ordered from top to bottom by the drugs having the most APDc/FPDc prolongation to the most APDc/FPDc shortening at the clinical Cmax concentration when averaged among the four combinations of platform and cell type.

Fig. 4

216x258mm (300 x 300 DPI)

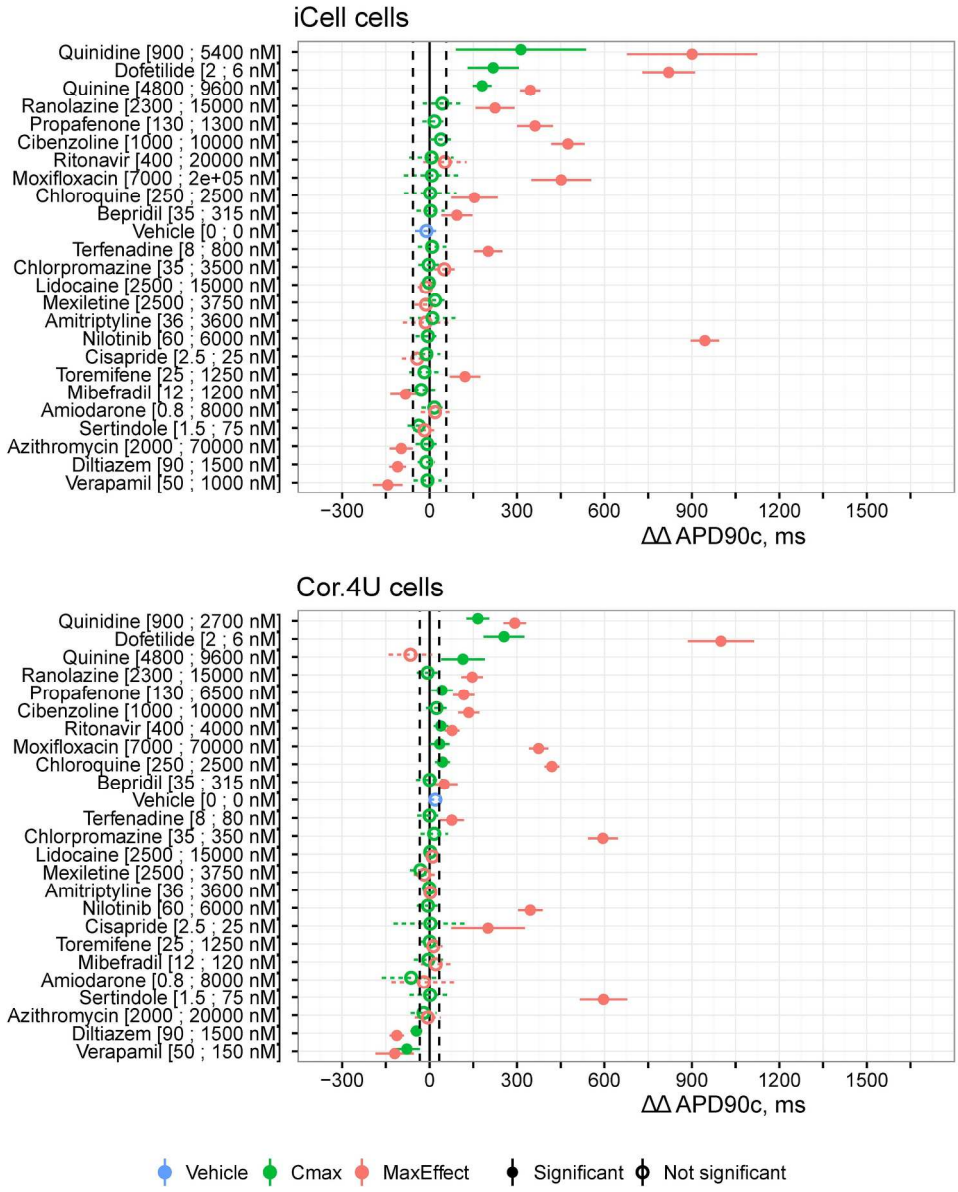

Fig. 5. Acute effects of 25 drugs on APD90c in iCell and Cor.4U cardiomyocytes
The two panels represent drug effects on APD90c in each cell type. The mean values for ΔΔAPDc are shown with the error bars representing 95% CI of the calculated mean across replicates (solid error bars are used for p-value <0.05, and dotted error bars are used for p-value≥0.05). The effect on APD90c at clinical Cmax (green) and the maximum effect observed at any drug concentration (red) are shown for each drug. Note that only drug doses when APD90c could be measured (i.e. cells were spontaneously beating and the induced arrhythmias did not interfere with the APD90c calculations) are included. The vertical black dotted lines represent 2 SD threshold calculated for the variability in APD90c for the vehicle control wells for each cell type. The drugs are ordered from top to bottom by the drugs having the most APD90c/FPDc prolongation to the most APD90c/FPDc shortening at the clinical Cmax concentration when averaged among the four combinations of platform and cell type.

Fig. 5
215x255mm (300 x 300 DPI)

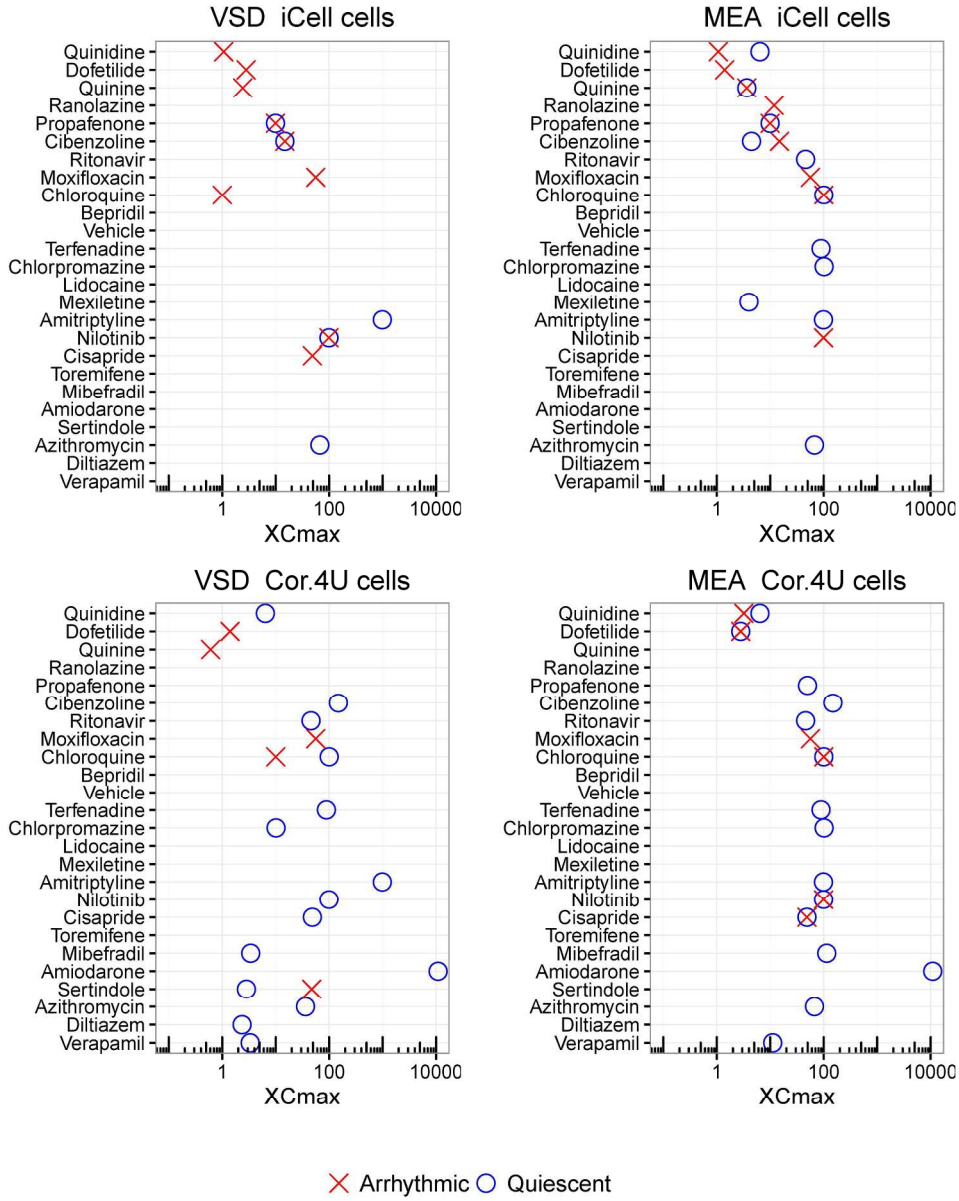

Fig. 6. Drug induced arrhythmias/quiescence in iCell and Cor.4U cardiomyocytes
The four panels represent drug-induced arrhythmias and inhibition of the spontaneous beating (quiescent) effects in each cell type-assay combination. The lowest drug concentration at which drug-induced arrhythmias (red crosses) or cessation of spontaneous beating (blue circles) is shown for each drug as number of folds of the clinical Cmax of that drug.

Fig. 6
219x266mm (300 x 300 DPI)

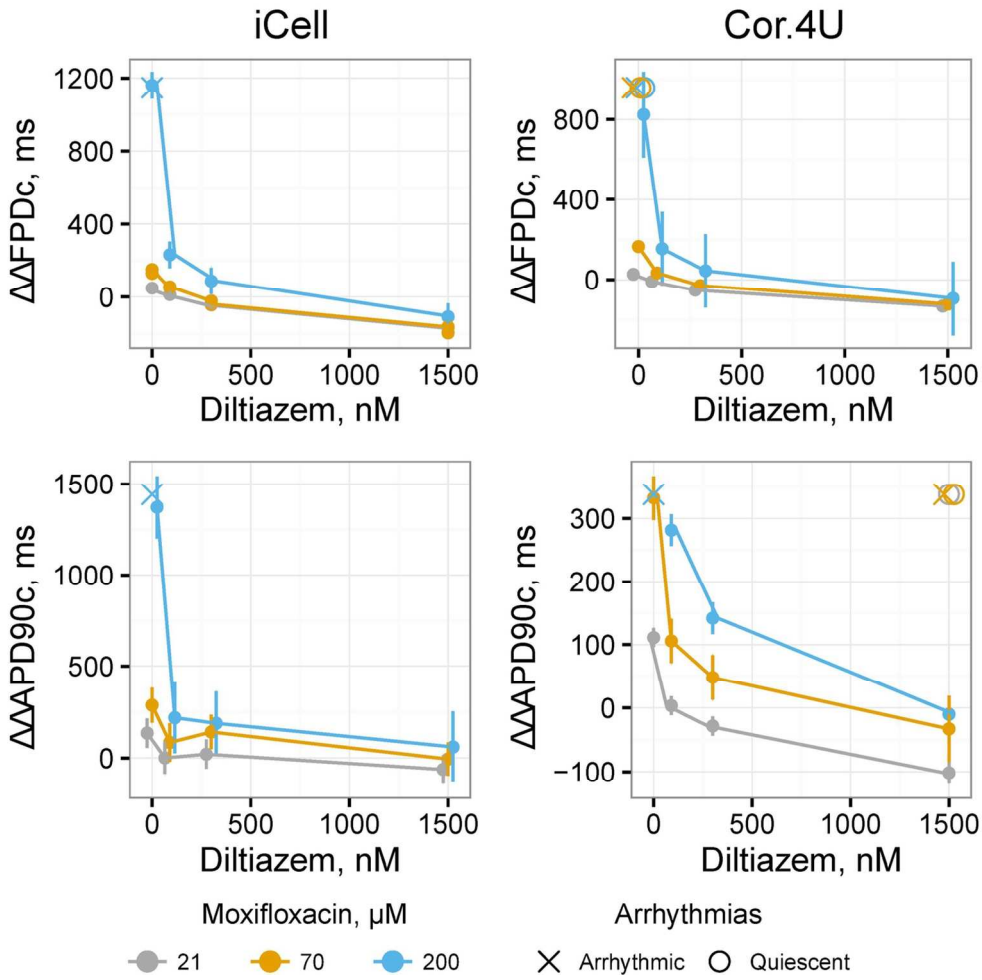

Fig. 7. Diltiazem effect on moxifloxacin-induced APDc/FPDc prolongation and arrhythmias
The four panels represent drug effects in each cell type/assay combination. Moxifloxacin was added to the iPSC-CMs at three different concentrations at the first dosing, then diltiazem was added in increasing concentrations at the three subsequent dosings while moxifloxacin concentration was maintained constant. The least-square means of drug-induced changes in FPDc and APD90c are shown with error bars representing 95% CI from the means. The symbols on the top of the graphs represent time points where either arrhythmias (open symbols) or inhibition of spontaneous beating (crosses) were observed. The color of the symbols corresponds to the color-coding of moxifloxacin concentrations (see the legend on the bottom of the plot).

Fig. 7
124x122mm (300 x 300 DPI)

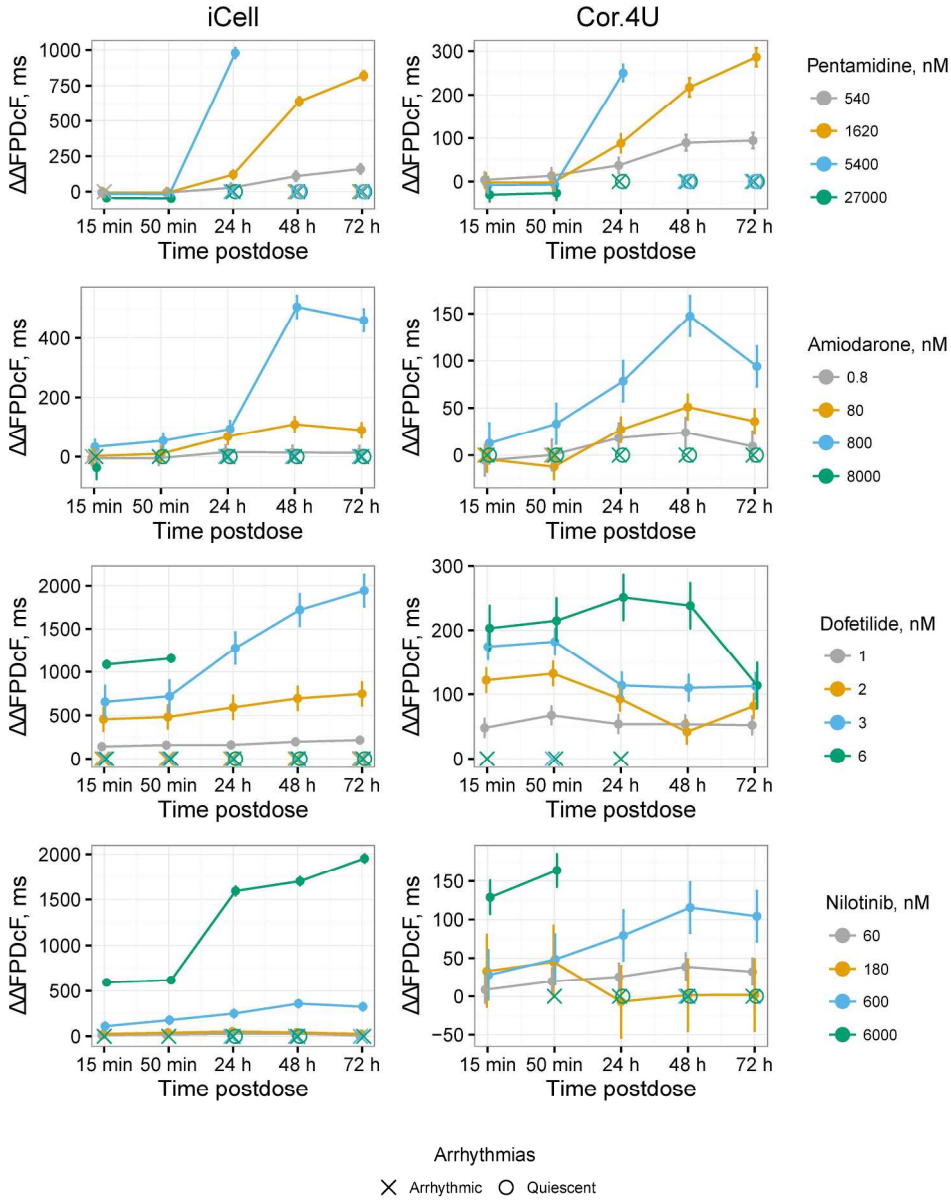

Fig. 8. Chronic effects of pentamidine, amiodarone, dofetilide and nilotinib on iCell and Cor.4U cardiomyocytes in MEA assay

The mean drug-induced changes in FPDc are shown with error bars representing 95% CI from the least-square means of the differences. The symbols on the bottom of the graphs represent time points where either arrhythmias (crosses) or inhibition of spontaneous beating (open circles) were observed. The color of these symbols corresponds to the color-coding of the drug concentrations (see the legend on the right side of each panel).

Fig. 8
221x277mm (300 x 300 DPI)